Chalcogenide Letters Vol. 11, No. 8, August 2014, p. 381 - 388

Fe(III) INDUCED STRUCTURAL, OPTICAL, MAGNETIC AND ELECTRICAL BEHAVIOR OF HYDROTHERMALLY SYNTHESIZED POLYVINYL PYRROLIDONE CAPPED CdS NANOPARTICLES

A. A. KUMAR[a], A. KUMAR[a*], J. K. QUAMARA[a], S. PRIYA[b]
[a]*Department of Physics, National Institute of Technology Kurukshetra, Haryana 136119, INDIA*
[b]*Center for Energy Harvesting Materials and Systems (CEHMS) Virginia Tech, Blacksburg, VA 24061, USA*

We report facile hydrothermal synthesis of polyvinyl pyrrolidone capped pristine and iron (Fe) containing cadmium sulfide (CdS) nanoparticles. The X-ray diffraction pattern of pristine CdS indicated the formation of wurtzite type hexagonal phase with space group $P6_3mc$ and lattice parameter a = 4.21 and c = 6.76Å; average crystallite size being ~ 12nm. The increase in Fecontent revealed cell volume contraction and decrease in crystallite size, due to resulted positive pressure on the lattice caused by smaller size and higher oxidation state of Fe^{3+}than Cd^{2+}ion. The bandgapwas found to decrease as 2.84, 2.75 and 2.55eV (for the Fe content of 0, 2 and 4 at%, respectively) due to Fe^{3+} induced $3d^3$ defect levels below the lowest unoccupied molecular orbitals of CdS. Photoluminescence spectra revealed redshift and decease in emission intensity with increase in Fe content. Fourier transform infrared spectra, transmission electron micrographs together with thermal analysis exhibited that pristine and Fe doped CdS nanoparticles were capped with polyvinyl pyrrolidone. Magnetic studies revealed weak ferromagnetic order in pristine CdS, which, was found to increase with increase in Fe induced t_{2g} defect levels. The electrical conductivity was found to increase with increase in Fe content.

(Received June 22, 2014; Accepted August 14, 2014)

Keywords: Nanoparticles, Hydrothermal, Cadmium sulfide, Photoluminescence, Room temperature ferromagnetism

1. Introduction

Cadmium sulfide (CdS) can possess cubic and/ or hexagonal phase. Thebulk CdSin hexagonal phase exhibits the band gap of ~2.4 eV, and technologically is one of the most important II-VI group semiconductor [1, 2]. The II-VI group semiconductors with incorporation of transition metal ions such as Mn, Ni, Fe, Co, Cr exhibit the enhanced magnetic spin order. The optical behaviour and band gap values also change due to additionaldefects levels introduced in the band gap on incorporation of these magnetic elements [3, 4]. These properties can further be engineered using nano-structuring.There are several reports ascribing the origin of ferromagnetic spin order to the substitution of magnetic atoms in CdS [5,6,7].The percentage of magnetic metal substitution has been found to exhibit a fine control over the magnetization, coercivity and remnantmagnetizationvalues. However, similar to pristine oxide nanomaterials, the pure CdS has also revealed ferromagnetic spin order. It has been suggested to arise due to cationic and surfacedefects[8].Therefore, the incorporation of magnetic metals at nanoscalemakestheinvestigation complex so as to understand if the observed spin order is due to magnetic metal substitution and/ or quantum size effects. It has already been found that the incompatibility of dopant with the host lattice because of the differences in size, crystal structure,

* Corresponding author: ashokku@nitkkr.ac.in

oxidation state, etc. put obstacle in the absorption of impurities on the nanoparticles surface [9].Further, the proper lattice site substitution will take place if the diffusion force of the dopant ions exceeds the self-purificationforce. This process can be controlledviananoparticle synthesis techniques, and, in turn, structural, optical, magnetic and electricalbehavior can be engineered.

The comprehensive study on Fe^{3+} induced structural, optical, magnetic and electric behaviorof CdS nanoparticles islacking[10,11].In present work, we report hydrothermal synthesis of polyvinyl pyrrolidone (PVP) capped pristine and Fe doped CdS nanoparticles. The Fe induced effects on structural, optical, magnetic and electrical behavior of PVP capped CdS nanoparticles will be investigated.

2. Experimental

Polyvinyl pyrrolidone cappedFe doped CdS (0, 2 and 4 at %) nanoparticles were prepared by hydrothermal method. Aqueous solutions of $Cd(NO_3)_2.4H_2O$ and required amount of Fe $(NO_3)_3.9H_2O$ were stirred for 30 min at room temperature then aqueous solution of sodium sulfide (Na_2S) was added drop wise to it, subsequently5 mM content of polyvinyl pyrrolidone was added to the above solution. The resulting solution was stirred for 1 h, transferred afterward in a 100 ml Teflon- lined stainless steel autoclave and heated at 120^{o}C for 16 h. The autoclave was cooled to room temperature; the obtained product was filtered, ringed several times with ethanol, and subsequently dried for 4 h at 100^{o}C to obtain the polyvinyl pyrrolidonecapped Fe doped CdS (0, 2 and 4 at %) nanoparticles.

The phase of the synthesized samples was obtained by X-ray diffractometer(RigakuMiniFlex) using Cu-$K_{\alpha1}$ radiation with the wavelength (λ) as 1.54056 Å with a scanning rate of 1^o/min (in the range 2θ = 20-80). Diffuse reflectance spectra were recorded by using UV-Visible double beam spectrophotometer (Camspec M550) in the spectral range of 400-700 nm. Photoluminescence spectra were collected in the wavelength range 430-700 nm with the excitation wavelength of 390 nm using Shimadzu RF-530 spectrofluorometer. Raman spectra in the range of 120–1000 cm^{-1}were obtained on aLABRAM HR 800 micro Raman spectrometer with a solid-state laser excitation at 633 nm.Magnetization measurements were carried out using vibrating sample magnetometer (VSM, Microsense Easy model EV9) and resistivity was measured using Vander Pauw method (Marine model SMU 01).

3. Results and discussions

3.1 Structural and phase analysis

The X-ray diffraction (XRD) patterns of synthesized PVP capped Fe (0, 2, 4 at.%) doped CdS nanoparticles are shown in the Fig (1). The observeddiffraction peaks at 2θ values of 24.11, 25.6, 27.07, 42.9, 50.92, 69.4 and 71.5^{o}for pristine CdScorrespond to the Bragg planes (1 0 0),(0 0 2), (1 1 0), (1 1 2), (2 1 1) and (1 1 4), respectively. The diffraction peaks with Fe incorporation shift slightly towards higher 2θ values.The XRD patterns of the samples are broadened progressively with Fe content indicating decrease in crystallite size with Fe incorporation. The ionic radius of Fe^{3+}(0.69 Å) is smaller than Cd^{2+}(0.96 Å), which exerts positive pressure on the crystal lattice, and, in turn, reduces the crystallite size. The lattice constant values for pristine CdS are estimated as a = 4.21 and c = 6.76Å, which are in good agreement with the known values (JCPDS # 77-2306). These values decrease with increase in Fecontent.The incorporation of Fe in CdS lattice results in the lattice contraction, as the ionic radius of $Fe^{3+}$is smaller than that of Cd^{2+}. All samples exhibited pure hexagonal phase with no traces of any secondary phase.

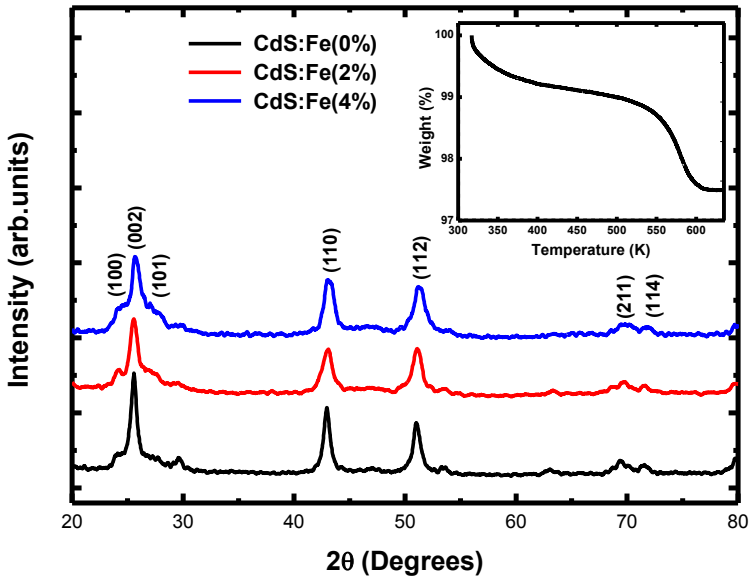

a)

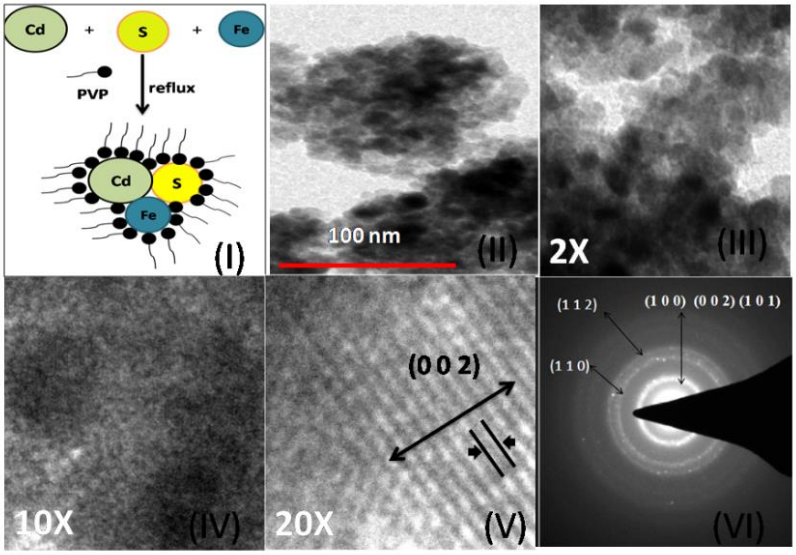

b)

Fig. 1(a) (Color online) X-ray diffraction pattern of PVP capped CdS nanoparticles with Fe content of 0, 2 and 4 at. %; inset shows the thermo-gravimetric analysis of CdS nanoparticles, (b)(I)- Schematic of growth mechanism forpolyvinyl pyrrolidone capped CdS nanoparticles,(II-IV)Transmission electron micrographs under different magnificarions,(V) lattice fringe pattern and(VI) Selected area electron diffraction pattern of CdS nanoparticles.

The average crystallite size (D) of the synthesized nanoparticles has been calculated by using Scherrer's formula, $D = 0.9\lambda/\beta\cos\theta$, where λ is the wavelength of X-ray used, β is the full-width at half maximum and θ is the Bragg angle. The values of D were found to be 12, 10 and 8 nm, for the samples with Fe content of 0, 2 and 4 at.%, respectively. Inset of Fig (1(a)) shows the thermo-gravimetric analysis of PVA capped CdS nanoparticles performed in nitrogen ambient in the temperature range of 300- 635 K at the heating rate of 2^{o}/min. This shows the total weight loss

of about 2.4%; indicating the removal ofPVP from the capped CdS nanoparticles.The two stages of the weight loss are clearly visible 300- 500 K and 500- 610K. Initial weight loss occurs due to removal of adsorbed water. At the second stage the weight loss is rapid and takes place due to the decomposition and removal of PVP. The incorporation/capping of PVP on CdS nanoparticles has further been discussed using transmission electron micrographs, Fourier transform infrared, and Raman spectroscopy in following paragraphs.

Growth mechanism of PVP capped CdS nanoparticles is illustrated in Fig (1b (I)).Fig (1b (II-IV)) shows the TEM micrograph of pristine CdS nanoparticles at different magnifications. The morphology of all the samples is found to be spherical. The crystallites are surrounded by polyvinyl pyrrolidone which acts as a capping agent. The average diameter ofthe nanoparticles is 11 nm, which is in good agreement with the estimated size from the XRD pattern. Fig (1(b) V) represents the TEM image of the single crystal oriented in the direction of [0 0 2] with lattice spacing of 0.33 nm. Fig (1b (VI)) shows the selected area electron diffraction(SAED) pattern of CdS nanoparticles.This shows wurtzite-type structure and matches well with the X-ray diffraction analysis.

Fig 2. (a)shows the Fourier transform infrared (FTIR) spectra of pristine and Fe doped CdS nanoparticles. The peaks observed at 3397 cm^{-1} and 1632 cm^{-1} represents the O-H stretching vibrations of the water molecule indicating the presence of water on the surface of nanoparticles. The peaks at 1381 were due to aromatic stretching and the peak at 1134 cm^{-1} is due to C-O stretching which is commonly observed in PVP samples [12]. The O-H stretching and C-C aromatic peaks of Fe doped CdSwere blue shifted and intensity was found to decrease. The absorption peak at 621 cm^{-1} is ascribed to C-H stretching. It is evident from the FTIR analysis that CdS particles are coated with PVP. The inset of Fig. 2(a)shows the Raman spectra of PVP capped pristine and Fe doped CdS nanoparticles. The Raman peaks observed at 295, 585 and 895 cm^{-1}, respectively correspond to 1LO, 2LO, 3LO optical phonon modes in CdS and are in good agreement with reported values [13]. The peaks of Fe doped CdS nanoparticles are slightly red shifted in comparison withpristineCdS nanoparticles. The redshift is observed due to the small ionic radius of Fe in comparison with the Cd^{2+} ion, as the Fe^{3+} ions tend to occupy the substitutional cationic sites resulting in surface defects in lattice.

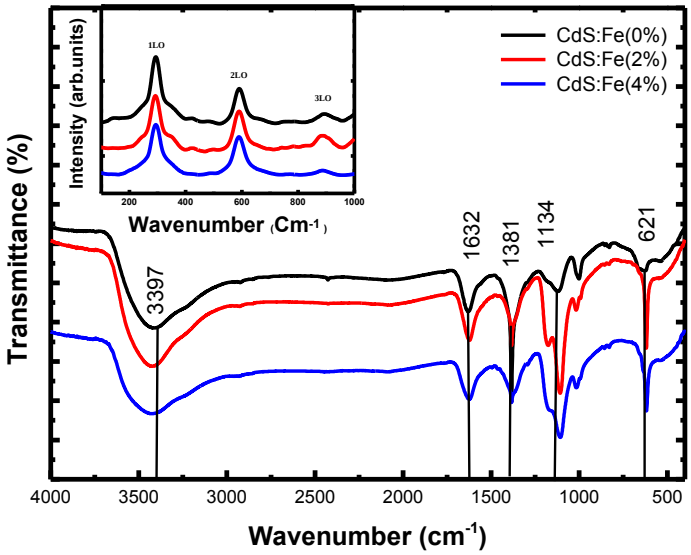

a)

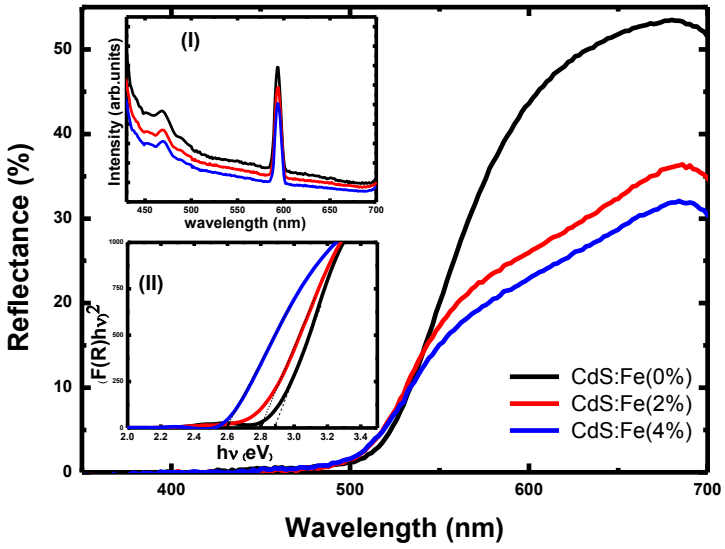

b)

Fig. 2(a) (Color online) Fourier transform infrared spectra of PVP capped CdS nanoparticles with Fe content of 0, 2 and 4 at. %; inset shows the Raman spectra of pristine and Fe doped CdS nanoparticles and (b) Diffuse reflectance spectra of pristine and Fe doped CdS nanoparticles; top left cornerinset (I) shows the photoluminescence spectra, and bottom left corner inset (II) shows plots for bandgap estimation.

3.2 Optical characterization

Diffuse reflectance spectra of polyvinyl pyrrolidone capped pristine and Fe doped CdS nanoparticles are illustrated in Fig. 2(b). The spectra were studied without taking into account the transmission losses. The bandgapvalues of the samples were estimated from diffuse reflectance spectra by plotting the square of the multiple of energy (hν) and of the Kubelka–Munkfunction F (R) versus hν, and subsequently extrapolating the linear part of the curve at F $(R)^2$= 0 [14].This has been shown in bottom left corner inset (II) of Fig. 2(b). The bandgap energy valuesfor PVP capped CdS nanoparticles were found to be 2.84, 2.75 and 2.55 eV for the Fe content of 0, 2 and 4

at. %, respectively.These show blue-shift of 0.42, 0.33and 0.13eV, respectively from bulk bandgapvalue of CdS at room temperature (2.42eV) [15]. This blue shift in energy is a direct consequence of the quantum confinement effect.Moreover, the incorporation of Fe^{3+} in CdS lattice has shown decrease in crystallite size while the bandgap approach toward the bulk values with increase in Fe content. This may be understood as follows. In CdS, the Cd^{2+} ions are in tetrahedral symmetry with S^{2-} ions. On occupying the Cd^{2+} lattice sites, the 3d orbital of Fe splitsinto two degenerate e_g (lower energy), and three degenerate t_{2g} orbitals (higher energy). As such Fe^{3+} introduces a low-lying unoccupied three energy states (LUMO level) $^3T_1$, $^5T_2$ and 5Ein the band gap, which, in turn, reduces the bandgap[16].

Top left corner inset (I) of Fig. 2(b) shows the room temperature photoluminescence spectra of PVP capped pristine and Fe doped CdSnanoparticles recordedat the excitation wavelength of 390 nm. The two peaks at 460(2.64 eV) and 590 nm (2.1 eV)are clearly observed in the photoluminescence spectra.The peak centered at 460 arises due to band-edge emission [17]. On incorporation of Fe^{3+} in CdS lattice, the peaks reveal redshift and decrease in intensity.The intermittent energy levels introduced near the conduction band act as LUMO level, and, in turn, exhibit the redshift in emission energy.The crystallite size also decreases with increase in Fe^{3+} content; revealing the increase in surface states. The increased surface states contribute toward the reduction of emission intensity due to increased trap levels. The cadmium vacancies and interstitial sulfur has also been observed in CdS, which contributetoward the decrease in emission intensity [18]. The Fe^{3+} has higher charge than Cd^{2+} and, therefore, the charge balance may create Cd vacancies and push sulfur to interstitial positions, and, in turn, cause the reduction in emission intensity [19].The yellow emission band centered about 590 nm is associated with the radiative transitions arising due to Cd atoms at the interstitial sites (Cd_i) as reported before by Lozada-Morale et al. [20].

3.3 Magnetic measurements

The magnetic measurements of PVP capped pristine and Fe doped CdS nanoparticles were performed at room temperature using vibrating sample magnetometer (VSM). Fig (3(a)) represents the M-H curves of pristine and Fe doped CdS nanoparticles with magnetic field ranging from -20 to 20 kOe. The pristine sample shows weak ferromagnetic behavior and Fe doped CdS nanoparticles exhibit increase in ferromagnetic order with saturated magnetizationbeing 0.02 and 0.05 emu/g for Fe content of 2 and 4 at. %, respectively; coercivity valuesbeing as 54.44 and 43.95 Oe, respectively. The origin of ferromagnetism in Fe doped CdS is of two possible ways, the first one is the formation of secondary phase such as ferrous oxide [21]. In the present work, no impurity phase was observed which can be confirmed from XRD and/or Raman analysis. In II-VI semiconductor nanomaterials, the nature of magnetic properties depends on the magnitude of transition metal ion exchange couplings with the electronic levels of the host lattice. The weak ferromagnetism was observed in pristine CdS nanoparticles, which is observed due to the surface charge defects [22]. Theoretical report predicts that the Cd^{2+} vacancies can also give rise to the magnetic ordering in pristine CdS [23]. The presence of Cd^{2+} vacancies has also been confirmed in Section 3.2 through photoluminescence behavior. The magnetic properties of Fe doped CdS are modified because of the sp-d exchange interactions between localized d-electrons of the dopant and the mobile charge carriers in the host lattice. The F-center formation in these DMS nanoparticle is responsible for the magnetic ordering of these systems. The increasing trend observed in the lattice parameters with increase in the doping concentration depicts the increase in the defect ion concentration [24]. In the Fe doped CdS nanoparticles, if Fe^{3+} occupies the Cd^{2+} site , the charge imbalance between the host Cd^{2+} and Fe^{3+} results in the formation of defects in the CdS lattice [25]. In the present study, the F center is the sulfur vacancy with a trapped electron, the trapped electron overlaps with the d orbital of transition metal ion, As Fe is having $3d^6$ spin states, it will have the unoccupied spin orbitals, which are accessible for the exchange of trapped electron and the trapped electron will align anti- parallel to the dopant ion spins leads to the ferromagnetic coupling between two atoms [26].

a)

b)

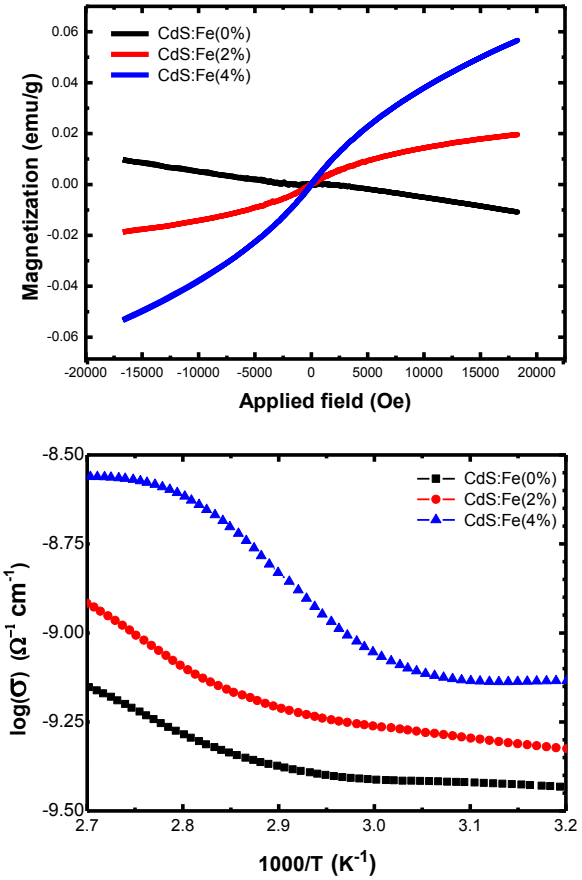

Fig. 3(a) (Color online) M-H curves and (b) Arrhenius plot showing the variation of electrical conductivity with temperature for pristine and Fe doped CdS nanoparticles.

3.4 Conductivity measurements

The electrical properties of pristine and Fe doped CdS nanoparticles were measured by using dc two probe method. The room temperature dependent electrical conductivity for pristine and CdS:Fe (2, 4 at%) is observed as 3.6 x 10^{-10} Ω^{-1} cm^{-1}, 4.7 x 10^{-10} Ω^{-1} cm^{-1}, 7.269 x 10^{-10} Ω^{-1} cm^{-1},respectively. Fig (3b) represents the variation of logarithm of conductivity (log (σ)) with the reciprocal of temperature for the pristine and Fe doped CdS nanoparticles. From the Fig (3b) it is observed that the electrical conductivity increases with temperature, indicating the semiconducting nature of the samples. The electrical conductivity increases with doping concentration as well, as a result of increase in the defects in the band region of CdS which acts as charge carriers. The activation energy of pristine and Fe doped CdS nanoparticles can be calculated by using the following equation,

$$\sigma = \sigma_0 e^{(\frac{-E_a}{KT})} \quad (1)$$

Where σ is the conductivity, σ_0 is the pre exponential factor, E_a is the activation energy, k is the Boltzmann constant and T is absolutetemperature. The activation energy for 0,2 and 4 at. % Fecontenthas been estimated as 0.18, 0.24 and 0.36 eV, respectively.

4. Conclusions

The polyvinyl pyrrolidone (PVP) capped pristine and Fe doped CdS nanoparticles were successfully synthesized by facile hydrothermal method using PVP as a capping agent, and

cadmium nitrate, sodium acetate and ferric nitrate as precursors for Cd, S and Fe, respectively.X-ray diffraction patterns revealed the formation of hexagonal phase for CdS nanoparticles with crystallite size in the range of 8-12 nm. The thermo-gravimetric analysis, Fourier transform infrared spectroscopy and transmission electron microscopy revealed the presence of polymer capping onCdSnanoparticles. The Raman spectra of the CdS nanoparticles showed the peaks at 292,589,893 cm^{-1} corresponding to the first, second and third order longitudinal optical phonon modes of CdS. The Fe doped CdS nanoparticles exhibit the slight redshift compared to that of pristine CdS which is attributed to the optical phonon confinement. Diffuse reflectance spectra has shown the redshift in the bandgap. The emission peaks at 460 and 590 nm were observed in the photoluminescence spectra of pristine and Fe doped CdS nanoparticles. The room temperature ferromagnetism was observed in pristine and Fe doped CdS nanoparticles. The Conductivity found to increase with the increase in the doping concentration.

Acknowledgement

This work was supported by SERB, Government of India (SERB/F/1769/2013-2014).

References

[1] M. Morkel,L. Weinhardt, B. Lohmuller, C. Heske, E. Umbach, W. Riedl, S. Zweigart, F. Karg, Appl. Phys. Lett.**79**, 4482 (2001).
[2] J. Zhang, F. H. Jiang, L. D. Zhang, J. Phys. Chem. B**108**, 7002 (2004).
[3] A. E. Morales, E. S. Mora, U. Pal, Rev. Mex. Defisica S**53**, 18(2007).
[4] P. Roy, S. K. Srivastava, J. Appl. Phys.**39**, 4771 (2006).
[5] P. Srivastava, P. Kumar, K. Singh, J. Nanopart Res. **13**,5077 (2011).
[6] S. Delikanli, S. He, Y. Qin, P.Zhang, H. Zeng, H. Zhang, M. Swihart, Appl. Phys. Lett. **93**, 132501 (2008).
[7] X. J. Wu, D. Z. Shen, Z. Z. Zhang, J. Y. Zhang, K. W. Liu, B. H. Li, Y. M. Lu, D. X. Zhao, B. Yao, Appl. Phys. Lett.**89,** 262118 (2006).
[8] Z. Yang, Z. Gao, Z. J. Zhu, Z. Shi, Z. Zhang, D. Xue, Nanoscale Res. Lett.**8**, 17 (2013).
[9] L. Levy; J. F. Hochepied; , M. P. Pileni J. Phys. Chem.**100**, 18322 (1996).
[10] G. Murali, A.D. Reddy, B. P. Prakash, R. P. Vijayalakshmi,B. K.Reddy,R. Venugopal, Physica B**407**, 2084 (2012).
[11] K. Kaur, G. S. Lotey, N. K. Verma, J. Mater. Sci. **25**, 2605 (2014).
[12] K. S. Kumar, A. Divya, P. Sreedhararedy, Appl. Surf. Sci.**257**, 9515 (2011).
[13] S. Chandramohan, A. Kanjilal, S. N. Sarangi, S. Majumder, R. Satyamoorthy,T. Som, J. Appl. Phys. **106**, 063506 (2009)
[14] A. E. Morales, E. S. Mora, U. Pal, Rev. Mex. Defisica S**53**,18 (2007).
[15] N. V. Hullavard, S. S. Hullavard, K. P. C. Arulkar, J. Nanosci. Nanotechnol. **8**, 3272 (2008).
[16] A. M. Liu, F. Q. Liu, H. Q. Guo, Z. G. Wang, Solid State Commun. **115**,615 (2000).
[17] L. Saravanan,A. Pandurangan,R. Jayavel, J. Nanoparticle Res. **13**,1621 (2011).
[18] V. Singh, P. Chauhan, J. Phys. Chem. Solids**70**,1074 (2009).
[19] J. H. Zhan, X. G. Yang, D. W. Wang, S. D. Li, Y. Xie, Y. Xia,Y. Qian, Adv. Mater **12**, 1348 (2000).
[20] R. L. Morales, O. Z. Angel, G. T. Delgado, Appl. Phys. A**73**, 61 (2001).
[21] A. Sundaresan, C. N. R. Rao, Nano Today **4**, 96 (2009).
[22] J. P. Tang, L. L. Wang, H. J. Luo, W. Z. Xiao, Phys. Lett. A**377**, 572 (2013).
[23] D. Chakraborti, S. Ramachandran,G. Trichy, J. Narayan, J. Prater, T. J. Appl. Phys. **101**, 053918 (2007).
[24] S. Kumar, S. Kumar, S. Jain, N. K. Verma, Appl. Nanosci. **2**, 127 (2012).
[25] S. B. Singh, M.V. Limaye, S. K. Date, S. Gokhale, S. K. Kulkarni, Physical Rev. B. **80,** 235421 (2009).
[26] C. Madhu, A. Sundaresn, C. N. R. Rao, Phys. Rev. B.**77**, 201306 (2008).